PET tracers and techniques for measuring myocardial blood flow in patients with coronary artery disease

Bailing Hsu [✉]

Nuclear Science and Engineering Institute, University of Missouri-Columbia, Columbia, MS 65211, USA.

Abstract

Assessment of the relative distribution of myocardial flow with myocardial perfusion imaging (MPI) is methodologically limited to predict the presence or absence of flow-limited coronary artery disease (CAD). This limitation may often occur, when obstructive lesions involve multiple epicardial coronary arteries or disease-related disturbances of the coronary circulation coexist at the microvascular level. Non-invasive assessment of myocardial blood flow in absolute units with position emission tomography (PET) has been positioned as the solution to improve CAD diagnosis and prediction of patient outcomes associated with risks for cardiac events. This article reviews technical and clinical aspects of myocardial blood flow quantitation with PET and discusses the practical consideration of this approach toward worldwide clinical utilization.

Keywords: myocardial blood flow, PET, coronary artery disease

PET MYOCARDIAL PERFUSION TRACERS

So far, there are several myocardial perfusion radiopharmaceuticals qualified for PET flow imaging, such ^{15}O-water, ^{13}N-ammonia and ^{82}Rb. Differences in the first-pass extraction of these tracers determine their regional myocardial uptake in relation to regional blood flow (***Fig. 1***). Resting myocardial blood flow (MBF) measured with these tracers in healthy human is approximately 1.0 mL/(min • g) while MBF increases three fold or higher than 3.0 mL/(min • g) under pharmacological stress with adenosine or dipyridamole[1-3]. ^{15}O-water as an ideal myocardial flow tracer exhibits a linear relation to MBF over a wide range of flow rates while ^{13}N-ammonia and ^{82}Rb as two more commonly used tracers in routine clinical environment do not exhibit such a linear property[4]. Because of the non-linearity, roll-off of tracer uptake in the myocardium can result in underestimated calculation of regional myocardial blood flow at high flow levels. To accurately quantify MBF, it is necessary to apply proper physiological compensation for the non-linear relation between uptake and MBF.

Post intravenous injection, myocardial extraction fraction of ^{15}O-water approaches unity since its net uptake (the product of the first-pass tracer extraction) tracks linearly with myocardial blood flow[5-7]. To permit clinical utilization of ^{15}O-water with a short physical half-life of 125 seconds, an on-site cyclotron near a PET imaging system is required. Perfusion images of ^{15}O-water normally present low target to background ratios because of the phenomenon of equilibrated diffusion between adjacent water spaces (e.g. myocyte

[✉]Corresponding author: Bailing Hsu, Ph.D., Adjunct Professor, Nuclear Science and Engineering Institute, University of Missouri-Columbia. E2433, Engineering Building East, Columbia, MS 65211, USA. Tel/Fax: 1+978-319-0297/1-617-678-2530, E-mail: bailinghsu@gmail.com.
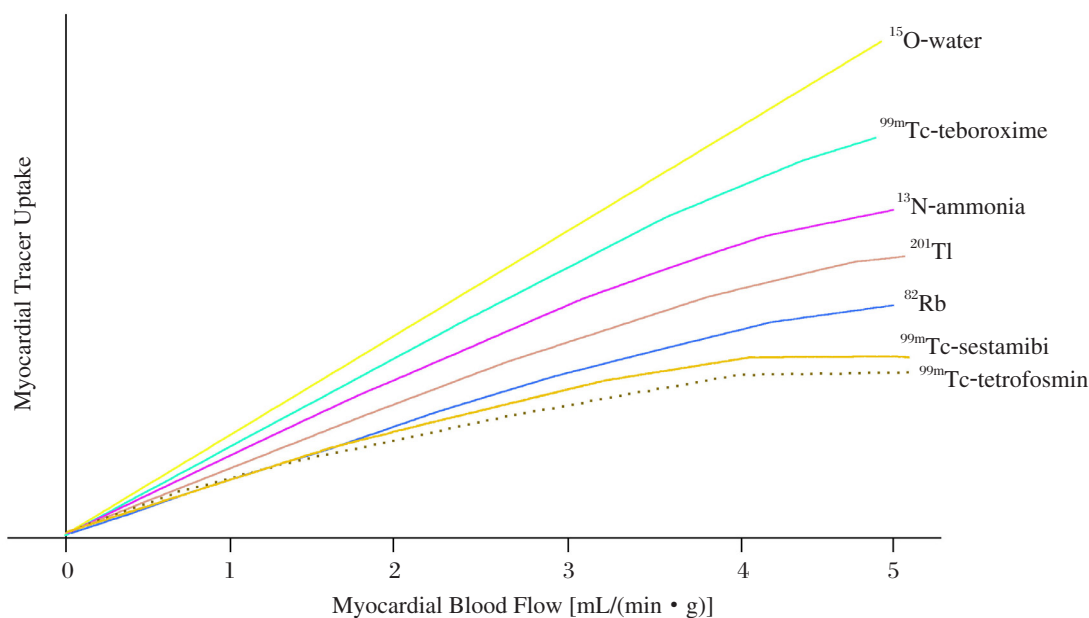
Fig. 1 Schematic illustration of radiotracer uptake in relation to regional myocardial blood flow.

and blood pool). ^{15}O-water is not typically used for assessment of myocardial perfusion alone, but mostly with measurements of MBF. Technically, the correction for high blood pool activity can be achieved by subtracting the images acquired from labeled arterial blood pool with inhalation of ^{15}O or ^{11}C carbon monoxide. However, the complexities of this procedure still encounter practical limitations for routine clinical utilization. Alternatively, novel analytical approaches based on factor analysis methods can be employed to simplify the process[8-10]. Since the measurement of MBF with ^{15}O-water PET is fairly accurate, it has been widely accepted as a non-invasive gold standard for flow assessment over several decades.

^{13}N-ammonia is another myocardial perfusion tracer delivered to the myocardium with intravenous injection and retained metabolically in the myocardium in proportion to MBF[11,12]. ^{13}N-ammonia exchanges across the capillary wall and transits through the interstitial spaces to reach the myocardial cell. Its first capillary transient retention fraction reaches about 85% for rest MBF but progressively and nonlinearly declines with increased blood flows. After entering myocyte, a fraction of tracer can diffuse back from tissue into blood while another fraction becomes metabolically trapped and retained in the myocardium through the α-ketoglutarate-to-glutamate and the glutamate-to-glutamine reactions[11]. Since the tracer is retained in the myocardium with rapid clearance from blood pool, perfusion images with high diagnostic quality can be obtained. High uptake in the lung and liver may also be observed in patients. In general,

over a few to ten minutes, ^{13}N-ammonia concentration in the myocardium remains retained before the loss of ^{13}N-labeled glutamine from the myocardium may occur. ^{13}N-ammonia´s physical half-life of 10 minutes permits repeated evaluations of rest and stress MBF at relatively short time intervals (about 30-40 minutes). Additionally, the tracer allows assessment of stress perfusion and left ventricular function with imaging protocols of treadmill exercise. Like ^{15}O-water, flow quantitation with ^{13}N-ammonia PET has also been widely accepted as another non-invasive gold standard for flow assessment. In fact, ^{13}N-ammonia is usually preferred rather than ^{15}O-water for qualitative evaluations of myocardial flow and perfusion images because of its superior image quality and simplified imaging protocols for clinical utilization. Nonetheless, because of the short physical half-life, ^{13}N-ammonia production still requires an on-site cyclotron.

Unlike ^{15}O-water and ^{13}N-ammonia, ^{82}Rb with an ultra short physical half-life of 75 seconds is a generator-produced myocardial perfusion PET tracer[13]. It is the decayed product from ^{82}Sr with a physical half-life of 28 days, which allows the clinical use of a generator system to produce ^{82}Rb for as long as 4 to 5 weeks. Since the biologic properties of ^{82}Rb as a positron-emitting cation are similar to those of potassium, intracellular uptake of ^{82}Rb across the sarcolemmal membrane can reflect the activity of cation transport via the Na-K ATPase transport system. When transported into myocyte, ^{82}Rb is retained in the myocardium in proportion to MBF. The first-pass retention fraction of ^{82}Rb reaches 65% for MBF at

rest but declines corresponding to higher flow rates. In patients with chronic CAD, myocardial uptake of [82]Rb is preserved in viable regions and largely reduced in scarred regions. In the setting of acute myocardial injury and reperfusion, initial uptake of [82]Rb can reflect the amount of recovered blood flow in revived area. Since necrotic myocardium cannot retain [82]Rb, the kinetics of [82]Rb washout may be utilized as an index of myocardial viability[14]. In the clinical setting, 40 to 60 mCi of [82]Rb is administered intravenously with a sophisticated infusion system to deliver targeted activities from the [82]Sr column[13]. After infusion of [82]Rb, data acquisition for perfusion images usually commences 60 to 120 seconds and continues for about 6 minutes[13,15]. Perfusion images with [82]Rb generally have a good diagnostic quality and can detect flow abnormalities with a similar accuracy to that of ^{13}N-ammonia[16,17]. However, patients with low left ventricular ejection fraction (LVEF) or severe lung disease may result in slower blood clearance to affect image quality. A general strategy to overcome this issue is to extend the waiting time beyond 120 seconds to collect perfusion data. Because of the ultra short physical half-life, infusion of high dose activities to attain statistically adequate images is generally necessary for [82]Rb PET imaging, but the high dose infusion, on the other hand, generates high count rates during the acquisition of input function. The over-exceeded count rates can lead to substantial dead-time losses for many current PET or PET/CT imaging systems, especially when they are operated in a 3D acquisition mode. Nevertheless, measurements of MBF in absolute units are still possible with low-dose protocols[18,19]. Because of the superiority of image quality and diagnostic accuracy over the traditional MPI[20] and the simplicity of on-site [82]Rb generator for clinical utilization, [82]Rb has been widely utilized in North America to clinically facilitate detection of CAD in patients suitable for pharmacological stress.

IMAGING METHODS

The high spatial and temporal resolutions of PET imaging with the capability of image quantitation are the essentials for MBF measurements. Rapidly acquired dynamic images (typically with 5-10 second frame rates) for several to ten minutes are necessary to track the initial transit of the radiotracer bolus through the central circulation and its continuous exchange from blood into the myocardium. In general, PET dynamic data acquisition should be started at least a few to ten seconds prior to the injection or infusion of PET tracers in order to establish the reference time point before tracer entering the imaging field of view. For stress flow measurement, it is crucial to inject PET tracers when the myocardium reaches the hyperemia stage with pharmacological stimulation or cold presser testing.

To produce quantitative dynamic images for accurate flow measurement, it is demanded to correct for physical interferences with in the PET images due to attenuation, scatter, randoms, and dead-time loss for high dose injection. Attenuation correction for dedicated PET systems are normally achieved by applying attenuation maps sequentially acquired by rotating multiple radionuclide rod sources (e.g. [68]Ge) or a single radioactive point source (e.g. [137]Cs) around patients. For PET/CT systems, separated low-dose CT images are acquired for the generation of attenuation maps. Quality control of misregistration and associated correction between emission images and attenuation maps acquired from either radionuclide transmission or CT is mandatory; otherwise, flow values would be systematically underestimated in regions with attenuation artifacts[21]. Scatter correction is generally achieved by modeling 511-keV scatter photons with reconstructed activity map of tracer distribution using the Monte-Carlo simulation process[22,23]. Randoms correction is usually applied to the sinogram raw data by estimating randoms in PET images based on singles rates measured for paired detector elements[24,25]. Compensation for the dead-time loss is important, particularly for high activity injection. It can be achieved by compensating singles count loss with the non-linear relation of singles count rate to activity presented in the imaging field of view. With all physical corrections applied, quantitative PET images with minimized physical interferences can be obtained. To depict the true regional radiotracer activity concentrations, pixel values in the corrected images are quantitatively presented in a physical unit of (Bq/mL). Quantitative images can be further employed to derive time activity curves of the arterial radiotracer input function and myocardial tissue response for flow calculation. In the process of quantitation, time activity curves are fitted with operational equations derived from tracer kinetic models (described below), which relate the externally observed tracer uptake to absolute MBF in the unit of mL//min/g through tissue kinetics. To utilize quantitative flow values for CAD detection, it is applicable to display regional estimates of MBF in the form of color-coded parametric images for clinical utilization[26].

PHYSIOLOGICAL FLOW MODELS

Among non-invasive medical imaging modalities for flow assessment, modeling tracer kinetics is a commonly used technique to simplify physiological proc-

ess of tracer uptake in mathematical terms for MBF calculation. Depending on the mechanism of tracer uptake from capillaries into myocyte, tracer kinetics can be described by one or two tissue compartments with multiple kinetic parameters as illustrated in *Fig. 2*. In general, ^{15}O-water and ^{82}Rb only require two kinetic parameters, K_1 (mL/min/g) and K_2 (min^{-1}), to calculate the rate of tracer uptake from blood to tissue and the rate of tracer washout from the tissue. ^{13}N-ammonia demands an additional parameter, K_3 (min^{-1}), to depict the rate of metabolic process in myocyte as previously described.

In the compartmental flow model consisting of K_1 and K_2[27,28], time activity curves derived from the left ventricular blood pool and myocardium are fitted into the flow equation as:

$$C_m(t) = FBV \cdot C_a(t) + (1\text{-}FBV) \cdot K_1 e^{-k_2 t} \otimes Ca(t)$$

where K_1 (ml/min/g) and K_2 (min^{-1}) are two kinetic parameters characterizing the rate of tracer uptake from the blood to the myocardium and the rate of tracer washout from the myocardium, respectively. $C_m(t)$ is the measured activity concentration in the myocardium obtained from PET images, assumed to consist of arterial blood input $C_a(t)$ and true myocardial uptake as a convolution of K_1, K_2 and $C_a(t)$. FBV is referred to the fractional blood volume in $C_m(t)$ coming from $C_a(t)$, and (1-FBV) is the rest of faction contributed from the myocardial uptake. By applying the curve fitting process, K_1, K_2 and FBV can be exactly solved into numerical values. MBF (mL/min/g) is then converted from K_1 with additional compensation for tracer extraction (E) in myocardium:

$$K_1 = MBF \cdot E = MBF \cdot (1\text{-}a \cdot e^{-\beta/MBF})$$

where α and β are physiological parameters derived from the effective capillary permeability surface (PS) area product (mL/min/g) accounting for nonlinear tracer extraction as a function of MBF[29,30]. The assumption in this model is consistent with the observed tracer extraction, which typically decreases with flow as previously described. To compensate for the physiological variance (e.g. hypertension or hypotension), rest blood flow is corrected for baseline heart rate and blood pressure by the factor of rate-pressure product/ (10,000 bpm×mm Hg). Coronary flow reserve (CFR) as the indicator of flow augmentation from rest to stress is calculated by stress to rest flow ratio.

The techniques for noninvasive flow estimates with compartmental modeling can accurately reflect regional MBF up to 5.0 mL/(min • g). Validation studies with the arterial reference microsphere technique in animal experiments have been reported to demonstrate equally accurate flow estimates for both ^{15}O-water and ^{13}N-ammonia[31,32]. More recently, a study with ^{82}Rb shows a similar linear correlation between the flow estimates by PET imaging and microsphere blood flows[33]. Importantly, measurements of regional MBF with PET at rest stage, as well as during pharmacologically stimulated hyperemia or with cold presser testing, are highly reproducible. This property was confirmed by repeated MBF measurements during the same study session or by repeated measurements within several days[34-36].

Depending on the time period to obtain sequential dynamic images, it is applicable to further simplify the compartmental model for flow calculation by utilizing image data only acquired within the early phase. This applicability is based on the assumption that the tracer washout and metabolic process do not yet occur during the early few minutes; thereby, the effects of k_2 and k_3 can be logically neglected. This simplified model is particularly suitable for ^{82}Rb and ^{13}N-ammonia with the given property of tracer retention in the myocardium[37]. The flow equation only accounting for tracer retention for flow calculation is:

$$K_1 = E \cdot MBF = P(t) / \int_0^t Ca(x)dx$$

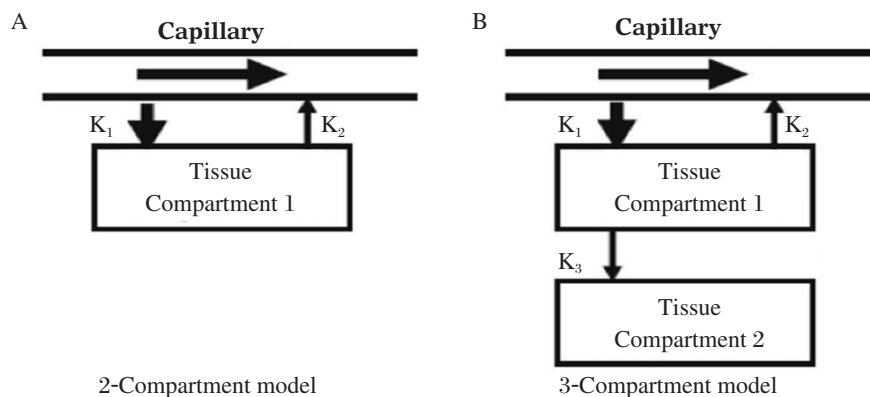where $P(t)$ is tracer uptake in the myocardium after

Fig. 2 Representative flow models. A: one-tissue compartment and two kinetic parameters as a two compartment model. B: two-tissue compartments and three kinetic parameters as a three compartment model.

time t, $\int_0^t Ca(x)dx$ represents the sum of arterial blood concentration from the start of tracer injection to time t, and E is the myocardial extraction fraction of tracer.

The advantage of retention flow model is its simplicity without the necessity of curve fitting process to obtain K_1; thereby, the method enhances the applicability of
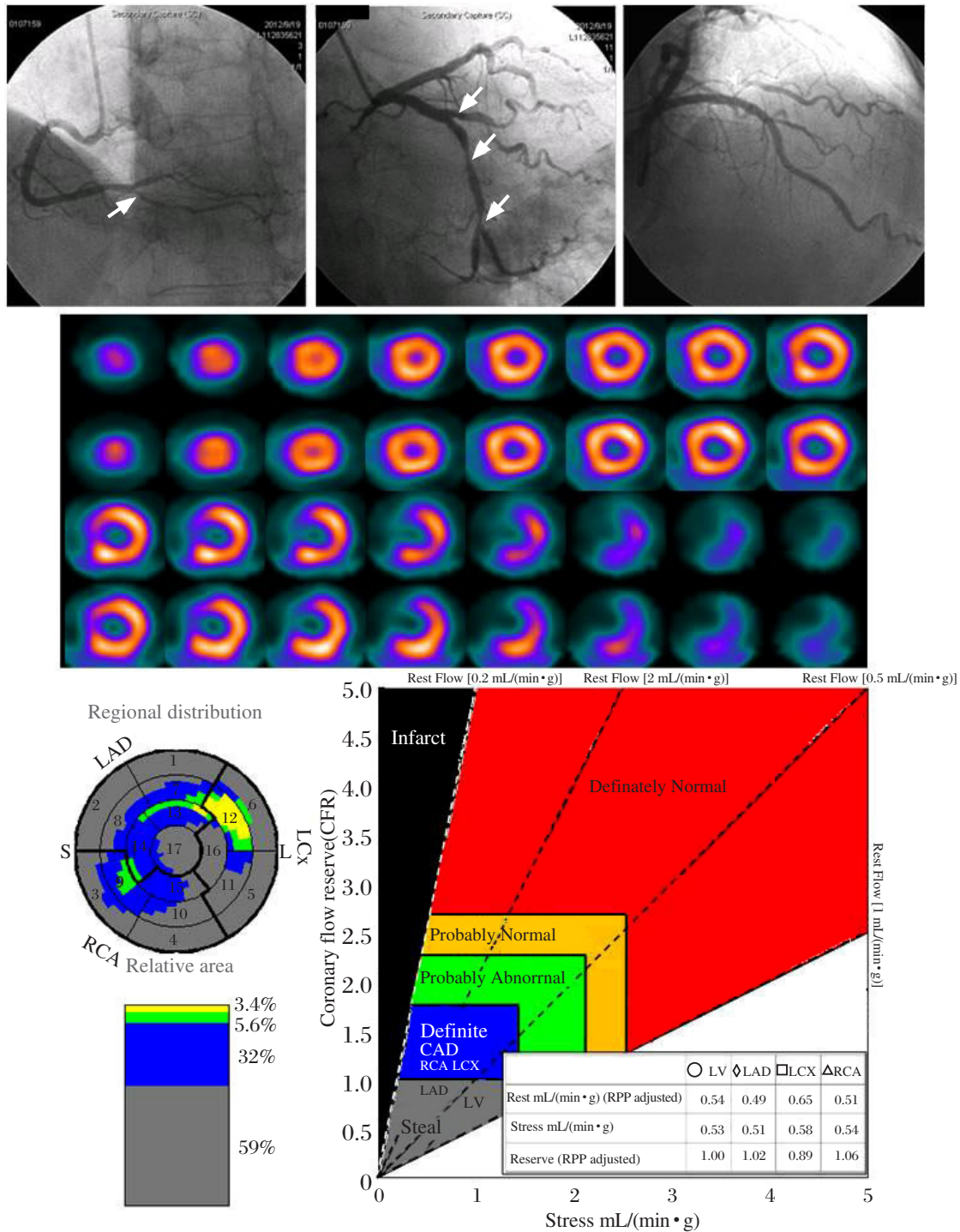

Fig. 3 An example of SPECT myocardial blood flow quantitation to detect three-vessel CAD with luminal narrowing in LAD. D1=90%; LCX: M=90%, D=90%, OM1=50%; RCA: PD=80%, confirmed by invasive coronary angiogram (upper panel). Attenuation-corrected perfusion images are interpreted to report a normal perfusion study without evidence of transient ischemia dilatation (middle panel). SPECT flow quantitation uncovers severe CAD with flow steal (CFR< 1.0) for all three territories associated with a total of 91% CAD burden throughout the whole myocardium (lower panel). LAD=left anterior descending, D1=diagonal 1, LCX=left circumflex, M=middle, D=distal, OM1=obtuse margina 1, RCA=right coronary artery, PD=posterior descending.

flow quantitation for routine clinical use. However, this simplified method utilizing a short period of data for flow calculation and lack of flexibility to accommodate for slow blood-pool clearance may be limited to calculate flow values for patients with low LVEF or severe lung problems.

CLINICAL APPLICATIONS OF PET FLOW QUANTITATION

Noninvasive assessment of absolute MBF in mL/(min • g) and CFR with PET is continuously emerging as a clinical tool to stratify risks for cardiac events and predict associated patient outcomes[38-40] and to evaluate the early stage of asymptomatic CAD[41,42]. Assessment of functional abnormalities of the coronary vessels with PET flow has an advantage over structural evaluation of the arterial wall. This advantage has been highlighted in classifying the early functional and progressive stages of coronary atherosclerosis before structural alteration within the arterial wall is magnified[43,44]. Consequently, adding PET flow information to the relative perfusion imaging provides incremental diagnostic value for CAD detection[45-47]. In addition, PET flow is an independent predictor of 3-vessel CAD[48,49] and a comprehensive tool to evaluate microvascular dysfunction with or without conventional cardiac risks[43,50,51]. The clinical integration of this approach has been recommended to enhance both CAD detection and risk assessment of patients with known or suspected CAD[52-54].

PRACTICAL CONSIDERATION

Although PET myocardial flow quantitation has been clinically marked as a powerful tool for diagnosis and prognosis of CAD, the utilization of PET flow as a routine clinical tool has several practical challenges. The main challenges come from general accessibility of PET flow tracers which are currently restricted to certain regions (e.g. North America and Europe), and the requirement of a relatively high cost to adopt in the clinical environment. Myocardial perfusion single photon emission computed tomography (SPECT) with ^{99m}Tc-labeled myocardial perfusion tracers, such as ^{99m}Tc-sestamibi and ^{99m}Tc-tetrofosmin, remains the clinical standard for MPI worldwide[55]. Flow quantitation with SPECT, when available, may be a simple solution to overcome PET´s challenges to warrant a widespread utilization. In fact, modern SPECT instrumentation has been improved to have high temporal resolution for dynamic data acquisition. In the past this unique capability has not yet been well investigated to design clinical protocols for dynamic SPECT flow quantitation. The implementation of iterative reconstruction technique with effective physical corrections[56,57], in addition to SPECT instrumentation, collectively affirms to explore the clinical potential of flow quantitation with dynamic SPECT imaging. **Fig. 3** demonstrates an example of SPECT MBF quantitation compared with the traditional perfusion and invasive coronary angiography for the detection of multi-vessel CAD.

From the clinical standpoint, the accessibility of SPECT flow quantitation as a comprehensive clinical tool can be considerably important to areas where a proper myocardial PET tracer for flow quantitation is not available (e.g. Asian countries). From the economical standpoint, the SPECT approach for flow quantitation demands a much smaller financial overhead than the PET approach, therefore SPECT flow quantitation may also be attractive in areas, where both PET and SPECT myocardial flow tracers are available (e.g. North America and Europe).

References

[1]   Schindler TH, Facta AD, Prior JO, Campisi R, Inubushi M, Kreissl MC, et al. PET-measured heterogeneity in longitudinal myocardial blood flow in response to sympathetic and pharmacologic stress as a non-invasive probe of epicardial vasomotor dysfunction. *Eur J Nucl Med Mol Imaging* 2006; 33: 1140-9.

[2]   Vermeltfoort IA, Raijmakers PG, Lubberink M, Germans T, van Rossum AC, Lammertsma AA, et al. Feasibility of subendocardial and subepicardial myocardial perfusion measurements in healthy normals with (15)O-labeled water and positron emission tomography. *J Nucl Cardiol* 2011; 18: 650-6.

[3]   Renaud JM, Dasilva JN, Beanlands RS, Dekemp RA. Characterizing the normal range of myocardial blood flow with (82)rubidium and (13)N-ammonia PET imaging. *J Nucl Cardiol* 2013; 20: 578-91.

[4]   Schindler TH, Schelbert HR. PET Quantitaton of Myocardial Blood Flow, In: ATLAS Of NUCLEAR CARDIOLOGY SECOND EDITION, Dilsizian V, Narula J, Braunwald E. Current Medicine LLC, Philadelphia USA, 2005, 67-95.

[5]   Bergmann SR, Fox KA, Rand AL, McElvany KD, Welch MJ, Markham J, et al. Quantification of regional myocardial blood flow in vivo with $H_2^{15}O$. *Circulation* 1984; 70: 724-33.

[6]   Bergmann SR, Herrero P, Markham J, Weinheimer CJ, Walsh MN. Noninvasive quantitation of myocardial blood flow in human subjects with oxygen-15-labeled water and positron emission tomography. *J Am Coll Cardiol* 1989; 14: 639-52.

[7]   Iida H, Kanno I, Takahashi A, Miura S, Murakami M, Takahashi K, et al. Measurement of absolute myocardial blood flow with $H_2^{15}O$ and dynamic positron-emission tomography. Strategy for quantification in relation to the partial-volume effect. *Circulation* 1988; 78: 104-15.

[8] Hermansen F, Ashburner J, Spinks TJ, Kooner JS, Camici PG, Lammertsma AA. Generation of myocardial factor images directly from the dynamic oxygen-15-water scan without use of an oxygen-15-carbon monoxide blood-pool scan. *J Nucl Med* 1998; 39: 1696-702.

[9] Wu HM, Hoh CK, Buxton DB, Kuhle WG, Schelbert HR, Choi Y, et al. Quantification of myocardial blood flow using dynamic nitrogen-13-ammonia PET studies and factor analysis of dynamic structures. *J Nucl Med* 1995; 36: 2087-93.

[10] Wu HM, Hoh CK, Choi Y, Schelbert HR, Hawkins RA, Phelps ME, et al. Factor analysis for extraction of blood time-activity curves in dynamic FDG-PET studies. *J Nucl Med* 1995; 36: 1714-22.

[11] Schelbert HR, Phelps ME, Huang SC, MacDonald NS, Hansen H, Selin C, et al. N-13 ammonia as an indicator of myocardial blood flow. *Circulation* 1981; 63: 1259-72.

[12] Schelbert HR, Phelps ME, Hoffman EJ, Huang SC, Selin CE, Kuhl DE. Regional myocardial perfusion assessed with N-13 labeled ammonia and positron emission computerized axial tomography. *Am J Cardiol* 1979; 43: 209-18.

[13] Gould KL. Clinical cardiac PET using generator-produced Rb-82: a review. *Cardiovasc Intervent Radiol* 1989; 12: 245-51.

[14] Gould KL, Yoshida K, Hess MJ, Haynie M, Mullani N, Smalling RW. Myocardial metabolism of fluorodeoxyglucose compared to cell membrane integrity for the potassium analogue rubidium-82 for assessing infarct size in man by PET. *J Nucl Med* 1991; 32: 1-9.

[15] Gould KL, Goldstein RA, Mullani NA, Kirkeeide RL, Wong WH, Tewson TJ, et al. Noninvasive assessment of coronary stenoses by myocardial perfusion imaging during pharmacologic coronary vasodilation. VIII. Clinical feasibility of positron cardiac imaging without a cyclotron using generator-produced rubidium-82. *J Am Coll Cardiol* 1986; 7: 775-89.

[16] Schelbert HR, Wisenberg G, Phelps ME, Gould KL, Henze E, Hoffman EJ, et al. Noninvasive assessment of coronary stenoses by myocardial imaging during pharmacologic coronary vasodilation. VI. Detection of coronary artery disease in human beings with intravenous N-13 ammonia and positron computed tomography. *Am J Cardiol* 1982 ;49: 1197-207.

[17] Demer LL, Gould KL, Goldstein RA, Kirkeeide RL, Mullani NA, Smalling RW, et al. Merhige ME. Assessment of coronary artery disease severity by positron emission tomography. Comparison with quantitative arteriography in 193 patients. *Circulation* 1989; 79: 825-35.

[18] Lortie M, Beanlands RS, Yoshinaga K, Klein R, Dasilva JN, DeKemp RA. Quantification of myocardial blood flow with 82Rb dynamic PET imaging. *Eur J Nucl Med Mol Imaging* 2007; 34: 1765-74.

[19] Prior JO, Allenbach G, Valenta I, Kosinski M, Burger C, Verdun FR, et al. Quantification of myocardial blood flow with 82Rb positron emission tomography: clinical validation with 15O-water. *Eur J Nucl Med Mol Imaging* 2012; 39: 1037-47.

[20] Bateman TM, Heller GV, McGhie AI, Friedman JD, Case JA, Bryngelson JR, et al. Diagnostic accuracy of rest/stress ECG-gated Rb-82 myocardial perfusion PET: comparison with ECG-gated Tc-99m sestamibi SPECT. *J Nucl Cardiol* 2006; 13: 24-33.

[21] Rajaram M, Tahari AK, Lee AH, Lodge MA, Tsui B, Nekolla S, et al. Cardiac PET/CT misregistration causes significant changes in estimated myocardial blood flow. *J Nucl Med* 2013; 54: 50-4.

[22] Ollinger JM. Model-based scatter correction for fully 3D PET. *Phys Med Biol* 1996; 41: 153-76.

[23] Watson CC, Newport D, Casey ME, deKemp A, Beanlands RS, Schmand M. Evaluation of simulation-based scatter correction for 3-D PET cardiac imaging. *IEEE Trans Nucl Sci* 1997; 44: 90-7.

[24] Watson CC, Casey ME, Bendriem B, Carney JP, Townsend DW, Eberl S, et al. Optimizing injected dose in clinical PET by accurately modeling the counting-rate response functions specific to individual patient scans. *J Nucl Med* 2005; 46: 1825-34.

[25] Walker MD, Matthews JC, Asselin MC, Saleem A, Dickinson C, Charnley N, et al. Optimization of the injected activity in dynamic 3D PET: a generalized approach using patient-specific NECs as demonstrated by a series of ^{15}O-H$_2$O scans. *J Nucl Med* 2009; 50: 1409-17.

[26] Johnson NP, Gould KL. Integrating noninvasive absolute flow, coronary flow reserve, and ischemic thresholds into a comprehensive map of physiological severity. *JACC Cardiovasc Imaging* 2012; 5: 430-40.

[27] Coxson PG, Huesman RH, Borland L. Consequences of using a simplified kinetic model for dynamic PET data. *J Nucl Med* 1997; 38: 660-67.

[28] Klein R, Beanlands RS, deKemp RA. Quantification of myocardial blood flow and flow reserve: Technical aspects. *J Nucl Cardiol* 2010; 17: 555-70.

[29] Renkin EM. Transport of potassium-42 from blood to tissue isolated mammalian skeletal muscles. *Am J Physiol* 1959; 197: 1205-10.

[30] Crone C. Permeability of capillaries in various organs as determined by use of the indicator diffusion method. *Acta Physiol Scand* 1963; 58: 292-305.

[31] Kuhle WG, Porenta G, Huang SC, et al. Quantification of regional myocardial blood flow using 13Nammonia and reoriented dynamic positron emission tomographic imaging. Circulation 1992; 86: 1004-17.

[32] Muzik O, Beanlands RS, Hutchins GD, et al. Validation of nitrogen-13-ammonia tracer kinetic model for quantification of myocardial blood flow using PET. *J Nucl Med* 1993; 34: 83-91.

[33] Lautamaki R, George RT, Kitagawa K, et al. Rubidium-82 PET-CT for quantitative assessment of myocardial blood flow: validation in a canine model of coronary artery stenosis 2009; 36: 576-86.

[34] Schindler TH, Zhang XL, Prior JO, et al. Assessment of

intra- and interobserver reproducibility of rest and cold pressor test-stimulated myocardial blood flow with (13) N-ammonia and PET. *Eur J Nucl Med Mol Imaging* 2007; 34: 1178-88.

[35] Siegrist PT, Gaemperli O, Koepfli P, et al. Repeatability of cold pressor test-induced flow increase assessed with H(2)(15)O and PET. *J Nucl Med* 2006; 47: 1420-6.

[36] Klein R, Renaud JM, Ziadi MC, et al. Intra- and inter-operator repeatability of myocardial blood flow and myocardial flow reserve measurements using rubidium-82 PET and highly automated analysis program. *J Nucl Cardiol* 2010; 17: 600-16.

[37] Yoshida K, Mullani N, Gould KL. Coronary flow and flow reserve by PET simplified for clinical applications using rubidium-82 or nitrogen-13-ammonia. *J Nucl Med* 1996; 37: 1701-12.

[38] Murthy VL, Naya M, Foster CR, Hainer J, Gaber M, Di Carli G, et al. Improved cardiac risk assessment with noninvasive measures of coronary flow reserve. *Circulation* 2011; 124: 2215-24.

[39] Ziadi MC, Dekemp RA, Williams KA, Guo A, Chow BJ, Renaud JM, et al. Impaired myocardial flow reserve on rubidium-82 positron emission tomography imaging predicts adverse outcomes in patients assessed for myocardial ischemia. *J Am Coll Cardiol* 2011; 58: 740-48.

[40] Herzog BA, Husmann L, Valenta I, Gaemperli O, Siegrist PT, Tay FM, et al. Long-term prognostic value of 13N-ammonia myocardial perfusion positron emission tomography added value of coronary flow reserve. *J Am Coll Cardiol* 2009; 54: 150-6.

[41] Czernin J, Barnard RJ, Sun KT, Krivokapich J, Nitzsche E, Dorsey D, et al. Effect of short-term cardiovascular conditioning and low-fat diet on myocardial blood flow and flow reserve. *Circulation* 1995; 92: 197-204.

[42] Dayanikli F, Grambow D, Muzik O, Mosca L, Rubenfire M, Schwaiger M. Early detection of abnormal coronary flow reserve in asymptomatic men at high risk for coronary artery disease using positron emission tomography. *Circulation* 1994; 90: 808-17.

[43] Camici PG, Crea F. Coronary microvascular dysfunction. *N Eng J Med* 2007; 356: 830-40.

[44] Reddy KG, Nair RN, Sheehan HM, Hodgson JM. Evidence that selective endothelial dysfunction may occur in the absence of angiographic or ultrasound atherosclerosis in patients with risk factors for atherosclerosis. *J Am Coll Cardiol* 1994; 23: 833-43.

[45] Muzik O, Duvernoy C, Beanlands RS, Sawada S, Dayanikli F, Wolfe ER Jr, et al. Assessment of diagnostic performance of quantitative flow measurements in normal subjects and patients with angiographically documented coronary artery disease by means of nitrogen-13 ammonia and positron emission tomography. *J Am Coll Cardiol* 1998; 31: 534-40.

[46] Hajjiri MM, Leavitt MB, Zheng H, Spooner AE, Fischman AJ, Gewirtz H. Comparison of positron emission tomography measurement of adenosine stimulated absolute myocardial blood flow versus relative myocardial tracer content for physiological assessment of coronary artery stenosis severity and location. *J Am Coll Cardiol Img* 2009; 2: 751-8.

[47] Fiechter M, Ghadri JR, Gebhard C, Fuchs TA, Pazhenkottil AP, Nkoulou RN, et al. Diagnostic value of 13N-ammonia myocardial perfusion PET: added value of myocardial flow reserve. *J Nucl Med* 2012; 53: 1230-4.

[48] Parkash R, deKemp RA, Ruddy TD, Kitsikis A, Hart R, Beauchesne L, et al. Potential utility of rubidium 82 PET quantification in patients with 3-vessel coronary artery disease. *J Nucl Cardiol* 2004; 11: 440-9.

[49] Ziadi MC, Dekemp RA, Williams K, Guo A, Renaud JM, Chow BJ, et al. Does quantification of myocardial flow reserve using rubidium-82 positron emission tomography facilitate detection of multivessel coronary artery disease? *J Nucl Cardiol* 2012; 19: 670-80.

[50] Graf S, Khorsand A, Gwechenberger M, Novotny C, Kletter K, Sochor H, et al. Typical chest pain and normal coronary angiogram: cardiac risk factor analysis versus PET for detection of microvascular disease. *J Nucl Med* 2007; 48: 175-81.

[51] Recio-Mayoral A, Rimoldi OE, Camici PG, Kaski JC. Inflammation and microvascular dysfunction in cardiac syndrome x patients without conventional risk factors for coronary artery disease. *JACC Cardiovasc Imaging* 2013; 6: 660-7.

[52] Schelbert HR. Quantification of myocardial blood flow: what is the clinical role? *Cardiol Clin* 2009; 27: 277-89.

[53] Schindler TH, Schelbert HR, Quercioli A, Dilsizian V. Cardiac PET imaging for the detection and monitoring of coronary artery disease and microvascular health. *JACC Cardiovasc Imaging* 2010; 3: 623-40.

[54] Schelbert HR. Positron emission tomography measurements of myocardial blood flow: assessing coronary circulatory function and clinical implications. *Heart* 2012; 98(7): 592-600.

[55] Vitola JV, Shaw LJ, Allam AH, Orellana P, Peix A, Ellmann A, et al. Assessing the need for nuclear cardiology and other advanced cardiac imaging modalities in the developing world. *J Nucl Cardiol* 2009; 16: 956-61.

[56] Zeintl J, Vija AH, Yahil A, Hornegger J, Kuwert T. Quantitative accuracy of clinical 99mTc SPECT/CT using ordered-subset expectation maximization with 3-dimensional resolution recovery, attenuation, and scatter correction. *J Nucl Med* 2010; 51: 921-8.

[57] Bailey DL, Willowson KP. An evidence-based review of quantitative SPECT imaging and potential clinical applications. *J Nucl Med* 2013; 54: 83-9.